portion of the boron s orbital is required in the cage bonding so that the orbital presented to the chlorine atom is predominantly of p character, and this allows a longer bond length than is afforded by sp^3 or sp^2 hybridization. The larger coupling constant is then due either to slightly less ionic character of the bond or a shift in hybridization of chlorine orbitals toward inclusion of less s character. That the boron s orbitals are usurped by the cage structure may be more pronounced in a chlorocarborane than in the parent carborane, as indicated by the shortened B–B bonds adjacent to the chlorine atom in the present case.

Acknowledgment.—We wish to thank J. Spielman and T. Onak for lending us the sample of 2-chloro-1,6-dicarbahexaborane(6). We are grateful for the unfunded computer time supplied by the USC Computer Center. The support of the United States Air Force Office of Scientific Research under Grant AFOSR 849-67 is gratefully acknowledged.

CONTRIBUTION FROM THE DEPARTMENT OF CHEMISTRY AND MATERIALS RESEARCH CENTER, NORTHWESTERN UNIVERSITY, EVANSTON, ILLINOIS 60201

Nature of the Donor–Acceptor Interaction in Boron Trihalide Complexes. Vibrational Spectra and Vibrational Analysis of Acetonitrile–Boron Trichloride and Acetonitrile–Boron Tribromide

BY D. F. SHRIVER*[1] AND BASIL SWANSON[2]

Received October 20, 1970

Infrared and Raman spectral data in the 4000–70-cm^{-1} region are reported for polycrystalline samples of $Cl_3B \cdot NCCH_3$ and $Br_3B \cdot NCCH_3$ at −196°. These data include five isotope species of each compound. In addition, Raman polarization data are presented for $Cl_3B \cdot NCCH_3$ in nitromethane solution. Normal-coordinate vibrational analyses based on constrained valence force fields show that the B–N stretching force constants follow the order $F_3B \cdot NCCH_3 < Cl_3B \cdot NCCH_3 \sim Br_3B \cdot NCCH_3$ (k(BN) = 2.5, 3.4, and 3.5 mdyn/Å, respectively). As with previous structural data, the force constants indicate a significantly stronger donor–acceptor bond for BCl_3 than for BF_3. These results require the abandonment of reorganization energy differences as the sole explanation of relative boron halide acidities. Alternate descriptions of the bonding were explored by CNDO/2 molecular orbital calculations on BF_3 and BCl_3. These calculations indicate that BCl_3 may have a higher electron affinity than BF_3.

Introduction

It is well known that the acidity of the boron halides, as judged by either free energy or heat of reaction, follows the order $BF_3 < BCl_3 \lesssim BBr_3$.[3] This trend is the opposite of that expected from electronegativity arguments, and the explanation generally offered is that the energy necessary to reorganize the planar boron halide to the pyramidal form is more important than inductive effects. Estimates of this reorganization energy along with the thermochemical data on complex formation lead to the conclusion that the boron–donor bond strength follows the order expected from electronegativities: $BF_3 > BCl_3 > BBr_3$.[4]

In contrast to the estimates of the nitrogen–boron donor–acceptor energies,[4] it was recently shown that BCl_3 forms a shorter and presumably stronger B–N bond with acetonitrile than does BF_3.[5] The present work was designed to check further the degree of B–N interaction by means of B–N force constant determinations.

Experimental Section

Infrared Spectra.—Calibrations of the Beckman IR-9 and IR-11 instruments employed in this work were checked with water and CO_2 bands and found to be within ±1.0 cm^{-1}. Spectra were collected at low temperatures[6] on samples which were annealed at *ca.* 0° or lower. The annealing was not performed at room temperature in order to avoid reaction with the KBr window material used for infrared-cell windows in the 4000–400-cm^{-1} region.

Raman Spectra.—The Raman data were collected with Spex 1400-II double monochromator and photon rate detection circuitry.[7] Data for $Cl_3B \cdot NCCH_3$ were obtained with 6328-Å He–Ne laser excitation (Spectra Physics Model 125); while for $Br_3B \cdot NCCH_3$ a more powerful Ar ion laser (Coherent Radiation Model 52) was employed at 5145 Å. The annealed solids were observed in a simple low-temperature cell.[8] Solutions of Cl_3BNCCH_3 were contained in an evacuable cell,[6] and depolarization ratios were calculated from peak areas.

In an attempt to obtain polarization data for $Br_3B \cdot NCCH_3$, the Raman spectrum was run for acetonitrile solutions. However, peak positions did not correspond to those of the pure solid, and the background gradually increased as the solution developed a yellow color. Apparently BBr_3 undergoes a drastic reaction with liquid acetonitrile; however we could find no evidence for the presence of BBr_4^- in this solution.[9]

(1) Alfred P. Sloan Fellow, 1967–1969.

(2) NDEA Fellow, 1968–1970.

(3) D. R. Martin and J. M. Canon, "Friedel–Crafts and Related Reactions," Vol. 1, G. A. Olah, Ed., Interscience, New York, N. Y., 1963, p 399; T. D. Coyle and F. G. A. Stone, "Progress in Boron Chemistry," Vol. 1, H. Steinberg and A. L. McCloskey, Ed., Macmillan, New York, N. Y., 1964, p 83.

(4) C. T. Mortimer, "Reaction Heats and Bond Strengths," Pergamon Press, New York, N. Y., 1962, p 111 ff.

(5) B. Swanson, D. F. Shriver, and J. A. Ibers, *Inorg. Chem.*, **8**, 2182 (1969).

(6) B. Swanson and D. F. Shriver, *ibid.*, **9**, 1406 (1970).

(7) I. Wharf and D. F. Shriver, *ibid.*, **8**, 914 (1969).

(8) D. F. Shriver, B. Swanson, and N. Nelson, *Appl. Spectrosc.*, **23**, 274 (1969).

(9) On the basis of infrared data C. D. Schmulbach and I. Y. Ahmed, *Inorg. Chem.*, **8**, 1414 (1969), suggested that BBr_4^- is present in dilute solutions of BBr_3 in acetonitrile. From the present results it appears that appreciable quantities of BBr_4^- are not present in our freshly prepared solutions. (However there is no doubt that some reaction, other than simple adduct formation, takes place when BBr_3 is dissolved in aetonitrile.) Several possible explanations of the disparity are as follows: (1) the sampling technique for Raman work is less susceptible to contamination from the atmosphere and does not involve contact with alkali halide window material; (2) the BBr_3 concentrations were different in the two studies; (3) our observations were confined to freshly prepared solutions because fluorescence developed upon aging.

Assignments

For both adducts the assignments were based primarily on C_{3v} molecular symmetry, for which 7 A_1 and 8 E modes are both infrared and Raman active, while 1 A_2 mode is inactive in both spectra. The designation of fundamentals is given in Table I. Certain features

TABLE I

NUMBERING AND APPROXIMATE DESCRIPTION OF THE FUNDAMENTAL VIBRATIONS FOR $Cl_3B \cdot NCCH_3$ AND $Br_3B \cdot NCCH_3$ (C_{3v} SYMMETRY)

	A₁ class (symmetric)			E class (asymmetric)	
ν_1	CH_3	str	ν_9	CH_3	str
ν_2	C≡N	str	ν_{10}	CH_3	def
ν_3	CH_3	def	ν_{11}	CH_3	rock
ν_4	C—C	str	ν_{12}	BX_3	str
ν_5	B—N	str	ν_{13}	NCC	def
ν_6	BX_3	str	ν_{14}	BX_3	rock
ν_7	BX_3	def	ν_{15}	BX_3	def
			ν_{16}	BNC	def
	A₂ class				
ν_8	torsion				

of the spectra are explained in terms of selection rules for the solid state. Both adducts crystallize in the centrosymmetric space group *Pnma*.[5,10] There are four molecules of the chloride adduct in the unit cell at sites of C_s symmetry[5] and presumably the same situation exists for the isomorphous bromide. The correlation table between free molecule (C_{3v}), site symmetry (C_s), and factor group symmetry (D_{2h}) has been given elsewhere.[6] The important correlations between free molecule and factor group are as follows: $A_1 \rightarrow A_g$, B_{3g}, B_{1u}, and B_{2u}; $E \rightarrow A_g$, B_{1g}, B_{2g}, B_{3g}, A_u, B_{1u}, B_{2u}, and B_{3u}. Thus, A_1 modes of the isolated molecule yield two Raman-active modes and two different infrared-active modes, while E symmetry species yield three infrared-active and four Raman-active modes for the crystal.

Unless stated otherwise, all data were collected on solid normal isotopic molecules at *ca.* −196°. Special isotopic substitution is designated by listing only the enriched isotope(s), *e.g.*, $^{10}BD = X_3{}^{10}B \cdot NCCD_3$.

$Cl_3B \cdot NCCH_3$ and $Br_3B \cdot NCCH_3$. 4000–800 Cm^{-1}.—In this region both $Cl_3B \cdot NCCH_3$ and $Br_3B \cdot NCCH_3$ exhibit fundamentals (Tables II–V) primarily associated with the acetonitrile portion of the molecule which is documented elsewhere.[6] Assignments for observed infrared and Raman frequencies are presented in Tables II–V and display spectra are given in Figures 1–4. Infrared spectra for the 2300–2400-cm^{-1} region contain the intense C≡N stretching frequency, ν_2, as well as a strong band attributed to $\nu_3 + \nu_4$ (CH_3 deformation + C—C stretch). As with other complexes of acetonitrile this combination band is rendered intense by Fermi resonance with ν_2.[6,11] For $Cl_3B \cdot NCCH_3$ the combination band $\nu_3 + \nu_4$ occurs at 2353 cm^{-1}, which is somewhat lower than ν_2. By contrast, the combination band is slightly higher in the case of $Br_3N \cdot CCH_3$, *viz.*, 2377 cm^{-1}. If the usual corrections for Fermi resonance are applied,[12] the corrected position

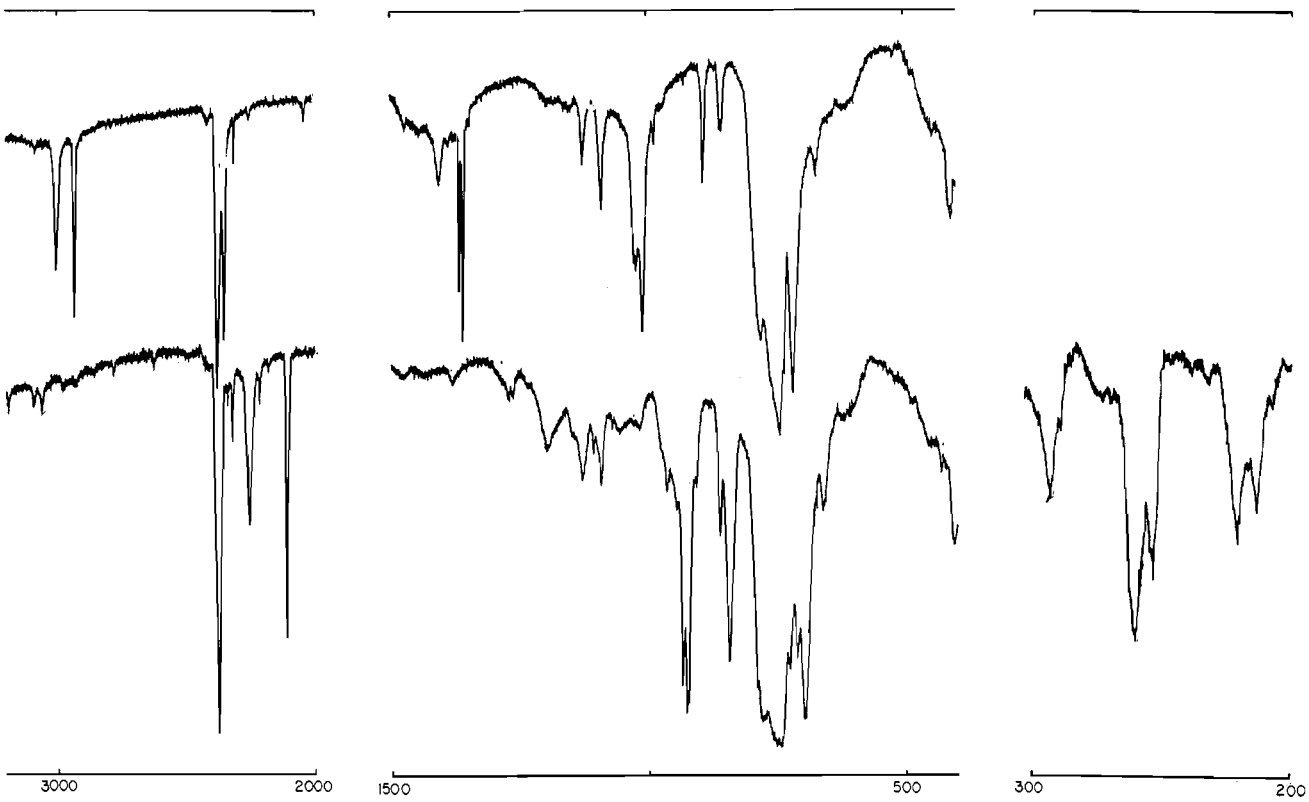

Figure 1.—Infrared spectra of $Cl_3B \cdot NCCH_3$ and $Cl_3B \cdot NCCD_3$ (cm^{-1}). The upper graph is the spectrum of $Cl_3B \cdot NCCH_3$ and the lower graph is the spectrum of $Cl_3B \cdot NCCD_3$ in all regions. The region below 450 cm^{-1} was scanned with the Beckman IR-11, and both spectra were taken using annealed samples at *ca.* −196°.

(10) S. Geller and O. N. Salmon, *Acta Crystallogr.*, **4**, 379 (1951); J. L. Hoard, T. B. Owen, A. Buzzell, and O. N. Salmon, *ibid.*, **3**, 130 (1950).

(11) J. C. Evans and G. Y.-S. Lo, *Spectrochim. Acta*, **21**, 1033 (1965).

(12) J. Overend in "Infrared-Red Spectroscopy and Molecular Structure," M. Davies, Ed., American Elsevier, New York, N. Y., Chapter 10.

TABLE II

OBSERVED INFRARED FREQUENCIES FOR $Cl_3B \cdot NCCH_3$ AT *Ca.* $-196°$ (cm^{-1})[a]

^{11}B[b]	^{11}BD[b]	$^{10}B^{15}N$	^{10}B	^{10}BD	Assignments
216 m	213 m	215 mw	216 m	213 m	ν_{15}
222 m	220 s	221 m	221 m	220 m	
259 m	252 s	257 vs	259 s	253 s	ν_{14}
266 vvs	260 vs	264 vs	266 vvs	260 vs	
287 w	292 m	310 vw	...	293 mw	ν_7
411 m	407 m	412 s	411 s	407 m	ν_6
417 m	412 m	416 m	417 s, sh	412 m	$2\nu_{15}$
~445 vw	430 vw	...	445 w	430 w	ν_{13}
...	~450 vw	...	...	~452 vw	$2\nu_{15}$
...	~620 w, b	...	...	~615 w, b	$\nu_6 + \nu_{15}$
672 w	660 m	669 mw	671 mw	661 mw	$\nu_6 + \nu_{14}$
...	...	...	...	694, 699 m	$\nu_6 + \nu_7$
...	...	...	...		
...	...	...	713 sh	...	?
...	712 s	717 s	721 m	...	$\nu_6 + \nu_7$
719 vs	698 vs	738 s	742 vs	714 vs	ν_5
...	727 s	...	759 s	730 vs	$\nu_7 + \nu_{13}$
...	...	752 s	...	743 m	$\nu_{10} - \nu_{14}$
746 vvs	750 vvs, b	...	...	...	ν_{12}
782 s	778 vs	775 vvs	777 vvs, b	774 vvs, b	$\nu_{12}(^{10}B)$
...	845 s	...	...	845 s	$\nu_{11}(D)$
856 w	...	848 m	857 m	...	$\nu_6 + \nu_{13}$
860 w	...	...	860 m	...	
892 m	862 m	870 m	893 m	862 m	$2\nu_{13}$
...	908 w	930 w	...	915 w	$\nu_5 + \nu_{15}$
...	926 vs	...	...	933, 937 vs	$\nu_4(D)$
...	939 s	...	...		$\nu_5 + \nu_{15}$
...	945 w, sh	...	...	...	$\nu_6 + \nu_{14}$
~975 vw	964 mw	...	...	964 mw	?
989 w	...	...	...	~982 w	?
...	~1015 vw	...	...	1016 w	$\nu_{10}(D)$
1010 s	...	1003 vs	1018 s	...	$\nu_4(H)$
1024 m	...	1025 s	1028 m	...	$\nu_{11}(H)$
...	...	...	...	1040 w	$\nu_{12} + \nu_{14}$
...	~1055 vw	...	...	1070 vw	$\nu_{15} + \nu_{11}$ or $\nu_7 + \nu_{12}$
1090 m	1091 mw	1090 w	...	~1092 vvw	$\nu_{11} + \nu_{16}(H)$, $\nu_{12} + \nu_{16}(D)$
...	1105 w	...	...	1106 w	$\nu_3(D)$
1127 mw	1127 mw	1125 w	1127 mw	1127 m	$\nu_5 + \nu_6$
...	~1147 w, sh	...	~1147 vw	...	?
...	...	...	...	1174 w	?
...	1198 mw	...	~1190 w	1199 vw, sh	$\nu_{12} + \nu_{13}$
...	...	...	...	1209 w	
...	1270, 1274 w	...	...	...	$\nu_{10} + \nu_{14}$
1357 s	...	1356 s	1357, 1364 ms	...	$\nu_3(H)$
1364 s	...	1363 s		...	
1403 m	...	~1390 m, b	1404 mw	...	$\nu_{10}(H)$
...	~1380 vw	...	...	~1420 vvw	$2\nu_5$
...	...	...	~1465 sh	...	?
...	~1477 vvw	~1500 m	~1530 vw	~1535 w	$2\nu_{12}$
~2042 vw	~1942 vvw	2045 w	2042 w	~1945 vw	$\nu_{10} + \nu_{11}(D)$, $2\nu_4(H)$
...	2110 s	...	...	2110 s	$\nu_1(D)$
...	2179 vvw	...	...	2180 vw	?
...	2214 w	...	...	2216 w	$2\nu_8(D)$
...	2252 m	...	...	2253 ms	$\nu_9(D)$
~2255 vvw	...	2285 m	...	...	$2\nu_{11} + \nu_{15}$
2312 w	2319 wm	...	2314 w	2319 wm	$\nu_3 + \nu_4 + \nu_7(D)$ or $2\nu_{11} + \nu_{14}$
...	2338 w	2344 sh	~2330 vvw	2339 w	$2\nu_3 + \nu_{16}(D)$, $2\nu_4 + \nu_7(H)$
2353 s	...	2360 s	2356 s	...	$\nu_3 + \nu_4$
2380 vs	2371 vvs	2329 vs	2381 s	2372 vs	ν_2
~2418 vvw	...	...	...	...	?
...	~2625 vw	...	...	~2620 vvw	$\nu_2 + \nu_6$
...	~2780 vvw	...	...	~2775 vvw	$\nu_1 + \nu_5$
2931 s	...	2926 s	2931 m	...	$\nu_1(H)$
3004 m	...	3004 ms	3003 m	...	$\nu_9(H)$
...	3058 vw	...	...	3075 vvw	$\nu_2 + \nu_4$
...	3090 vvw	...	...	3093 vw	$\nu_2 + \nu_5$
...	...	...	~3110 vvw	...	$\nu_2 + 2\nu_6$
...	3190 vw	...	...	3192 vvw	$\nu_1 + \nu_8$
...	3478 w	...	...	3479 w	$\nu_2 + \nu_3$

[a] These data represent spectra of annealed polycrystalline samples at *ca.* $-196°$. [b] Boron-11 indicates the normal isotopic distribution.

TABLE III

OBSERVED RAMAN FREQUENCIES FOR $Cl_3B \cdot NCCH_3$ AT *Ca.* −196° (cm^{-1})[a]

^{11}B[b]	^{11}B[b,c]	^{11}BD[b]	$^{10}B^{15}N$	^{10}B	^{10}BD	Assignments
78 s	...	78 m	...	79 s	79 s	ν_{16}
126 s	...	113 m	122 mw	123 m	119 ms	?
220 m	216 (0.8)	215 mw	221 ms	222 m	216 ms	ν_{15}
...	...	...	...	...	222 m, sh	
256 w	...	245 w	246 w	256 mw	252 w, sh	ν_{14}
263 m	258 (0.8)	257 w	264 mw	264 mw	260 m	
309 m	308 (0.73)	292 m	307 m	310 m	292 s	ν_7
...	...	404 w	...	...	402 vw	?
...	...	...	...	...	406 w	?
416 vs	410 (0.04)	409 vs	415 vs	415 vs	411 vs	ν_6
448 m	450 (0.8)	431 m	441 m	447 m	431 m	ν_{13}
706 m	699 (*ca.* 0.0)	684 w	724 mw	728 w	706 mw	ν_5
735 w	758 (0.78)	732 w	765 w	763 vw	762 w	ν_{12}
742 w		739 vw	772 w	772 vw	771 w	
...	...	...	785 w	787 vw	785 w	?
...	...	923 m	...	...	934 s	ν_4(D)
...	...	933 vw	...	...	939 w, sh	$\nu_5 + \nu_{15}$
...	1032 (*ca.* 0.8)	...	...	...	...	ν_{11}(H)
1010 mw	998 (0.06)	...	999 mw	1015 w	...	ν_4(H)
1353 m	...	1104 w	1353 ms	1354 m	1107 mw	ν_3(H)
...	...	2110 vs	...	...	2110 vs	ν_1(D)
...	...	2214 vw	...	...	2218 mw	$2\nu_3$(D)
...	...	2252 mw	...	...	2253 mw	ν_9(D)
2351 ms	2346 (0.16)	...	...	2356 w	...	$\nu_3 + \nu_4$(H)
2379 ms	2371 (0.15)	2368 m	2326 vs	2381 w	2371 s	ν_2
2929 s	...	...	2930 vvs	2930 s	...	ν_1(H)

[a] Observed Raman frequencies from annealed solid samples at −196°. [b] Boron-11 represents the normal isotopic distribution. [c] Spectrum of nitromethane solution. Depolarization ratios are in parentheses.

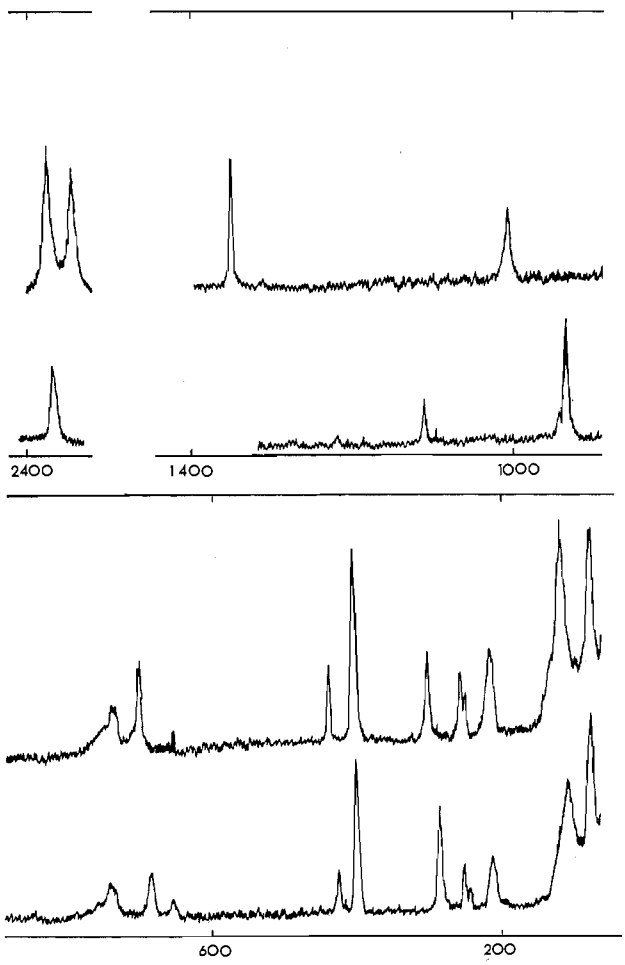

Figure 2.—Raman spectra of $Cl_3B \cdot NCCH_3$ and $Cl_3B \cdot NCCD_3$ (cm^{-1}). The upper graph is the spectrum of $Cl_3B \cdot NCCH_3$ and the lower graph is the spectrum of $Cl_3B \cdot NCCD_3$ in all regions. Both spectra were taken using the He–Ne 6328-Å exciting line and annealed samples at *ca.* −196°.

of ν_2 agrees well with that found for the deuterated molecules, where Fermi resonance is not a problem.

$Cl_3B \cdot NCCH_3$. 800–400 Cm^{-1}.—This region is dominated in the infrared spectrum by a very strong broad band which is centered at 746 cm^{-1} for the normal isotopic molecule (Figure 1) and is assigned to the asymmetric BCl_3 stretch, ν_{12}. The ^{10}B counterpart is observed around 780 cm^{-1}. In the Raman spectrum (Figure 2) this mode appears as a weak doublet at 742 and 735 cm^{-1} for the normal molecule; while in solution it appears as a single depolarized line at 758 cm^{-1}. The lack of correspondence between infrared and Raman frequencies and splitting in the Raman spectrum of the solid are understandable from the selection rules for the factor group.

Three other fundamentals in this region are $\nu_5(A_1$, B–N stretch), $\nu_6(A_1$, BCl_3 stretch), and ν_{13}(E, NCC deformation). The two symmetric modes are assigned to polarized bands at 699 and 410 cm^{-1} in the solution spectrum (Table III). Comparisons with $F_3B \cdot NCCH_3$[6] and $Br_3B \cdot NCCH_3$ (see below) indicate that the higher frequency mode around 700 cm^{-1} is the B–N stretch, ν_5. These symmetric modes are found at 719 cm^{-1} (ν_5) and 411 cm^{-1} (ν_6) in the infrared spectrum of the normal isotopic solid. The assignment of ν_5 is complicated by the occurrence of other strong peaks in the infrared spectrum around 700 cm^{-1}; however, isotopic shifts substantiate the current choice. The disparity between infrared and Raman frequencies for ν_{12} is attributed to factor group coupling.

The NCC deformation, ν_{13}, is assigned to very weak infrared bands at 445 and 430 cm^{-1} for the normal and D isotopic molecules, respectively. The magnitude of this isotopic shift agrees with that found for $F_3B \cdot NCCH_3$[6] and free acetonitrile.[13] As expected, this band is depolarized in the Raman spectrum of the solution.

(13) F. W. Parker, A. H. Nelson, and W. H. Fletcher, *J. Mol. Spectrosc.*, **1**, 107 (1957); W. H. Fletcher and C. S. Shoup, *ibid.*, **10**, 300 (1963).

TABLE IV

OBSERVED INFRARED FREQUENCIES FOR $Br_3B \cdot NCCH_3$ AT *Ca.* −196° (cm^{-1})[a]

^{11}B[b]	^{11}BD[b]	$^{10}B^{15}N$	^{10}B	^{10}BD	Assignments
...	106 vvw	...	...	112 vw, sh	?
128 s	121 m	129 m	129 m	120 m	?
143 m	143 m	143 m	142 m	142 m	ν_{15}
...	...	...	173 vw	172 vw	$\nu_{14} - \nu_{16}$
191 s	189 s	190 s	191 s	188 s	ν_7
266 vvw	250 w	...	...	249 w	ν_{14}
290 vvs	283 vs	288 vs	290 vs	283 vs	ν_6
429 vw	414 w, b	...	...	~415 w, b	ν_{13}
...	464 w, b	...	...	~460 w, b	$\nu_6 + \nu_7$
555 w	...	550 vvw	555 w	~532 vvw	$2\nu_6$
614 w	...	...	619 vw	~622 vvw	$\nu_7 + \nu_{13}$
...	...	653 m	654 ms	652 m	$\nu_6 + 2\nu_7$
659 vvs	658 vvs	...	...	...	ν_{12}
...	...	689 vvs	686 vvs	683 vvs	ν_{12}
690 vs	680 vs	699 vvs	693 vvs	...	ν_{12}
715 s	692 s	713 vs	719 vs	704 vvs	ν_5
...	...	728 sh	...	...	?
733 ms	...	738 s	737 s	...	$\nu_6 + \nu_{13}$
...	762 w	767 w	768 mw	765 mw	$2\nu_6 + \nu_7$
855 m	818 mw	843 m	858 m	819 mw	$2\nu_{13}$
...	837 ms	...	...	838 s	$\nu_{11}(D)$
...	...	...	...	925 ?	$\nu_6 + \nu_{12}$
~935 vvw	...	...	...	936 ?	$\nu_6 + \nu_{12}$
...	935 s	...	...	944 vs	$\nu_4(D)$
...	947 w	...	...	...	$\nu_5 + \nu_{14}$
992 w	964 w	...	968 w	971 w	$\nu_6 + \nu_5$
...	...	...	...	978 w	$\nu_6 + \nu_5$
...	1007 mw	...	...	1009 m	$\nu_{10}(D)$
1020 vs	...	1010 ms	1018 vs	...	$\nu_4(H)$
1022 vs	...	...	...	...	$\nu_4(H)$
1032 s	...	1018 sh	1032 s	...	$\nu_{11}(H)$
...	...	1023 sh	...	...	?
...	...	...	...	1042 vw	$\nu_{11} + \nu_{14}$
...	...	...	...	~1072 vw	$\nu_{12} + \nu_{13}$
~1125 vvw	...	...	1126 w	1090 vw	$\nu_5 + \nu_{13}$
~1195 vvw	...	...	1210 w	~1198	?
...	...	...	...	1248 vw	$\nu_{11} + \nu_{13}$
1348 m	...	1345 sh	...	...	$\nu_3(H)$
1353 s	...	1348 s	1348 s	...	$\nu_3(H)$
1360 m	...	1352 sh	1353 m	...	$\nu_3(H)$
1392 m	...	1390 ms	1391 w	...	$\nu_{10}(H)$
1446 w	...	1439 w	1446 w	...	$2\nu_5$ or $\nu_4 + \nu_{13}$
1475 sh	...	1500 w	...	...	?
2027 vw	...	2026 vw	2023 vvw	...	$2\nu_4$
2036 vw	...	...	...	...	$\nu_4 + \nu_{11}$
...	2106 mw	...	...	2108 m	$\nu_1(D)$
...	2246 mw	...	...	2248 mw	$\nu_9(D)$
...	...	2272 vw	...	...	?
2305 w	...	...	2306 vvw	2311 vw	?
2321 vw	...	...	...	2330 vw	$\nu_3 + \nu_5 + \nu_6$
2350 s	2362 s	2322 vs	2348 vs	2362 vs	ν_2
2377 s	...	2353 mw	2360 s	...	$\nu_3 + \nu_4$
...	...	...	2380 s	...	$\nu_3 + \nu_4$
...	2929 vw	...	...	...	$\nu_5 + \nu_9$
2922 m	...	2922 m	2922 s	...	$\nu_1(H)$
2997 m	...	2996 mw	2996 ms	...	$\nu_9(H)$
...	3040 vw	...	...	3058 vvw	$\nu_1 + \nu_4$
...	...	...	...	3075 vvw	$\nu_2 + \nu_5$
...	...	...	...	~3250 vvw	$\nu_2 + \nu_4$
...	...	...	...	3474 vvw	$\nu_2 + \nu_3$

[a] Spectra are reported for annealed samples. [b] Boron-11 indicates the normal isotopic distribution.

Possible assignments for overtone and combination bands are given in Table II.

400–50 Cm^{-1}.—One symmetric mode, $\nu_7(A_1, BCl_3$ deformation), is expected in this region. While the observed depolarization ratios (Table III) do not allow an unequivocal assignment, the 308-cm^{-1} band exhibits the lowest depolarization ratio (0.73). Comparisons with Clippard's definitive assignments in this region[14] also indicate that the infrared and Raman bands around 300 cm^{-1} should be assigned to ν_7.

(14) P. D. H. Clippard, Ph.D. Thesis, University of Michigan, 1969.

The two remaining depolarized bands at *ca.* 217 and *ca.* 260 cm^{-1} can be assigned to $\nu_{14}(E, BCl_3$ rock) and $\nu_{15}(E, BCl_3$ deformation), respectively. The normal-coordinate treatment (see below) supports the general correctness of this assignment but it also indicates that these modes are highly mixed. The splitting in ν_{14} and ν_{15} which occurs upon going from solution to the solid state is attributed to factor group effects in the solid.

As with $F_3B \cdot NCCH_3$,[6] the BNC deformation, ν_{16}, presents difficulties in assignment. Two bands which might be assigned to this mode are found around 120

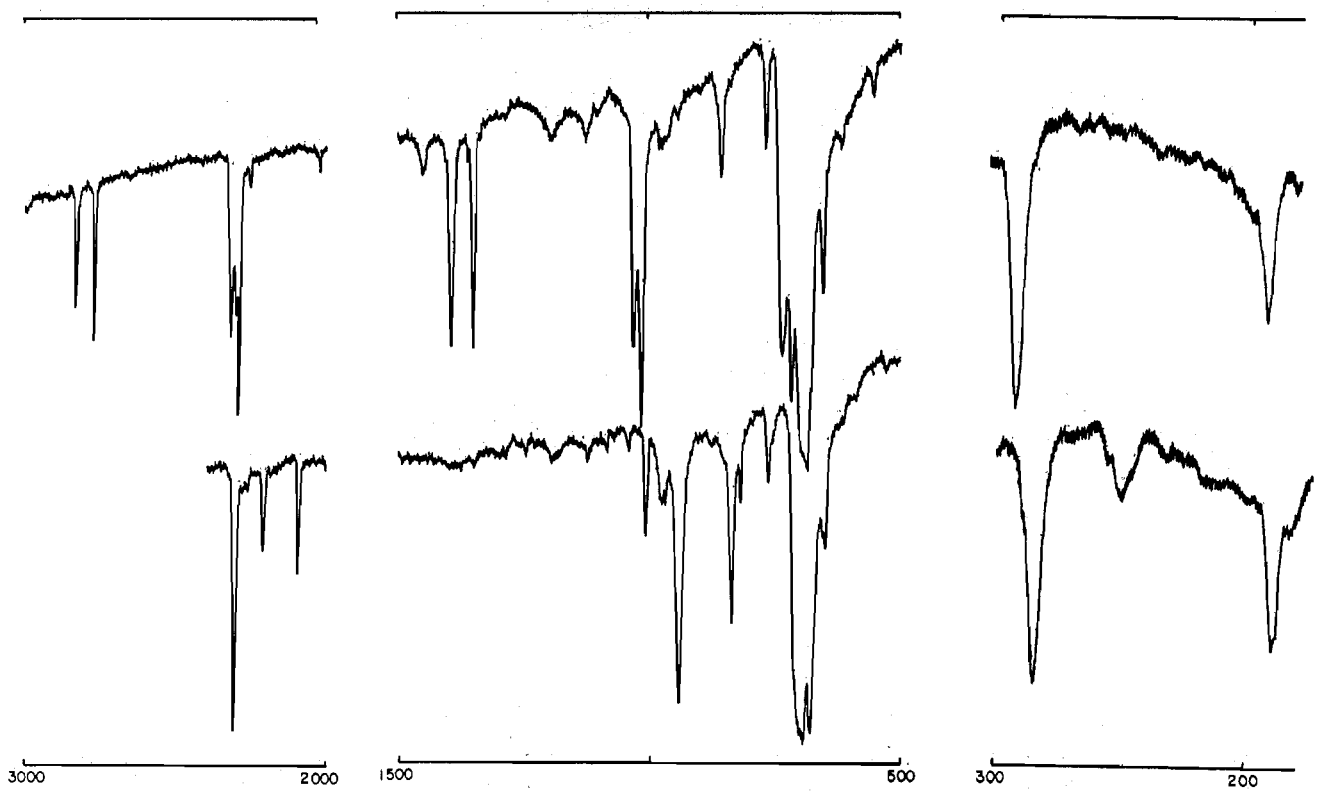

Figure 3.—Infrared spectra of $Br_3{}^{10}B \cdot NCCH_3$ and $Br_3{}^{10}B \cdot NCCD_3$ (cm^{-1}). The upper graph is the spectrum of $Br_3{}^{10}B \cdot NCCH_3$ and the lower graph is the spectrum of $Br_3{}^{10}B \cdot NCCD_3$ in all regions. The region below 450 cm^{-1} was scanned with the Beckman IR-11, and both spectra were taken using annealed samples at *ca.* −196°.

TABLE V

OBSERVED RAMAN FREQUENCIES FOR $Br_3B \cdot NCCH_3$ AT *ca.* −196° (cm^{-1})[a]

^{11}B[b]	^{11}BD[b]	$^{10}B^{15}N$	^{10}B	^{10}BD	Assignments
108 w, b	106 mw	108 mw	112 mw	115 m	?
...	116 w	127 vw	...	120 m	?
147 m	145 m	147 m	146 ms	144 m	ν_{15}
182 ms	180 ms	183 s	182 s	178 mw	ν_7
187 m	186 m	188 mw	188 m	190 s	ν_7
268 ms	251 m	267 m	266 m	248 m	ν_{14}
289 vvs	283 vs	289 vs	288 vs	281 vs	ν_6
403 m	...	397 m	...	...	?
426 m	408 mw	421 m	426 w	407 m	ν_{13}
642 ms	640 m	...	...	654 vw	ν_{12}
653 ms	652 m	670 m	671 m	669 mw	ν_{12}
690 w	692 vw, b	682 m	680 m	678 m	ν_{12}
700 ms	675 m	720 m	722 m	693 m	ν_5
...	934 s	...	...	943 s	$\nu_4(D)$
...	945 mw	...	...	...	$\nu_6 + \nu_{12}$
...	961 vw	...	...	...	$\nu_5 + \nu_6$
1019 vs	...	1004 m	1025 mw	...	$\nu_4(H)$
1030 mw	...	1018 m	...	...	$\nu_{11}(H)$
...	1014 w	...	...	1013 vw	$\nu_{10}(D)$
...	1106 w	...	...	1104 w	$\nu_3(D)$
1350 s	...	1352 vs	1350 mw	...	$\nu_3(H)$
...	...	1402 w	...	...	$\nu_{10}(H)$
...	2102 vs	...	...	2106 m	$\nu_1(D)$
...	2213 vvw	...	...	...	$2\nu_2$
...	2241 m	...	...	2241 w	$\nu_9(D)$
2349 ms	2362 vs	2318 vvs	2348 ms	2361 s	ν_2
2377 w	...	2361 w	2379 m	...	$\nu_3 + \nu_4$
...	...	2376 vw	...	...	$\nu_3 + \nu_4$
2914 vs	...	2315 vvs	2914 s	...	$\nu_1(H)$
2984 w	...	2987 mw	2985 w	...	$\nu_9(H)$

[a,b] See footnotes *a* and *b*, Table IV.

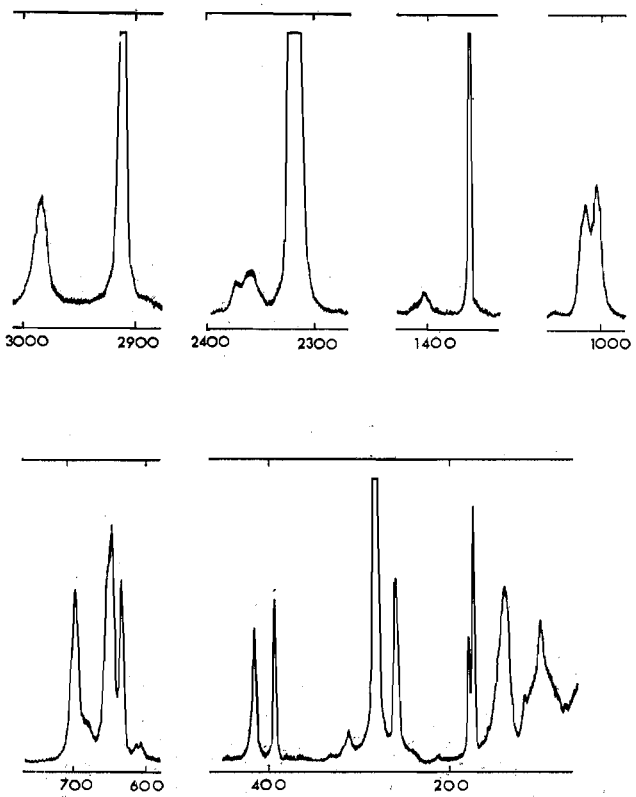

Figure 4.—Raman spectrum of $Br_3{}^{10}B \cdot NCCH_3$ (cm^{-1}). The spectrum was taken using the 5145-Å Ar ion exciting line and an annealed sample at *ca.* −196°

and 80 cm^{-1}. The lower frequency was finally chosen as ν_{16} for two reasons: (1) a satisfactory fit to the frequencies could not be obtained when the 120-cm^{-1} band was employed in the normal-coordinate treatment; (2) the absence of a frequency shift in the 120-cm^{-1} band when Cl is substituted for F. The low frequency assigned to this mode is reasonable in view of the weakness of the B–N bond. The ambiguity for this low-frequency assignment does not affect the symmetry

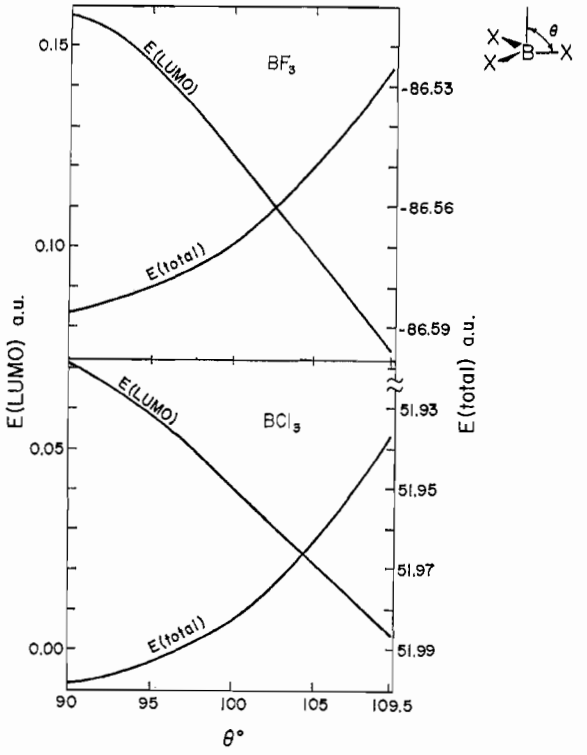

Figure 5.—Calculated energies for the lowest unoccupied molecular orbital E(LUMO) and the binding energies E(binding) *vs.* the degree of distortion. As illustrated $\theta = 90°$ corresponds to planar BX_3.

force constants belonging to the A_1 species and it has little or no influence on the valence force constants of primary interest (F_{BN}, F_{BCl}, and F_{CN}). Therefore, the principal conclusions of this work will not be affected if future experimental evidence leads to reassignment of the low-frequency region.

$Br_3B \cdot NCCH_3$. 800–400 Cm^{-1}.—The dominant feature in the infrared spectrum for the normal isotopic molecule is a very strong absorption centered around 659 cm^{-1} which is assigned to the asymmetric BBr_3 stretch, ν_{12} (Figure 3). This intense absorption along with the occurrence of several strong satellite bands complicates the assignment of the B–N stretch, ν_5, which is expected around 700 cm^{-1}. Fortunately, the Raman spectrum in this region (Figure 4) is much less complex than the infrared. The ^{10}B molecule exhibits a Raman line at 722 cm^{-1} which shifts to 700 cm^{-1} in the normal isotopic molecule and to 675 cm^{-1} in the D molecule. This pattern of isotopic shifts closely resembles that found for ν_5 in $Cl_3B \cdot NCCH_3$ and the *ca.* 700-cm^{-1} band is assigned accordingly. Two other prominent features occur at 680 and 671 cm^{-1} in the Raman spectrum of the ^{10}B molecule. These are assigned to two components of the asymmetric BBr_3 stretch, ν_{12}, which has been split by the low site symmetry of the molecule. The influence of the crystalline environment is also evident in the constant disparity between infrared and Raman bands for both ν_5 and ν_{12}. Similar effects are evident in the spectra of $Cl_3B \cdot NCCH_3$.

The remaining fundamental expected in this region is the NCC deformation, ν_{13}, which is assigned to a 429-cm^{-1} infrared band and 426-cm^{-1} Raman band in the spectra of the normal isotopic molecule. Isotopic shifts and the position of this band agree with those found for $F_3B \cdot NCCH_3$[6] and $Cl_3B \cdot NCCH_3$. Remaining features in this region are assigned to overtones or combination bands.

400–50 Cm^{-1}.—The symmetric BBr_3 stretch, ν_6, which is expected in this region may be assigned to the very strong infrared and Raman bands around 285 cm^{-1} (Figures 3 and 4). As with the corresponding vibration of $Cl_3B \cdot NCCH_3$, this mode is not significantly affected by isotopic substitution. Since polarization data on solutions were unobtainable, the symmetric BBr_3 deformation, ν_7, cannot be assigned with certainty. However, a reasonable assignment is *ca.* 190 cm^{-1} since the Raman spectra contain a sharp and intense doublet at this frequency. This agrees with the position of the corresponding mode for $Br_3B \cdot N(CH_3)_3$.[14] The band at *ca.* 145 cm^{-1} is attributed to the BBr_3 asymmetric deformation mode, ν_{15}, in agreement with the corresponding mode of $Br_3BN(CH_3)_3$.[14]

A band at *ca.* 250 cm^{-1} was originally considered to be too high to be any of the remaining fundamentals. Therefore, the BBr_3 rock, ν_{14}, was initially assigned to the band at 125 cm^{-1}. However, the normal-coordinate treatment using this assignment was unsatisfactory. The frequency fit and PED are reasonable when ν_{14} is assigned to the 250-cm^{-1} band. The high frequency for this normal mode appears to arise from extensive contributions from symmetry coordinates other than the BBr_3 rock (see below). Alternatively, the low-frequency peak of the doublet at *ca.* 190 cm^{-1} may be ν_{14}, the peak at *ca.* 143 cm^{-1} may be ν_{15}, and either or both of the peaks at *ca.* 125 and *ca.* 110 cm^{-1} may be ν_{16}. Since all of these frequencies fall in the E class, a change in assignments would have no effect on calculating the B–N stretching force constants and little or no effect on the other force constants of primary interest.

Calculation of Force Constants

Symmetry force constants were calculated using Schachtschneider's iterative least-squares program and associated programs.[15] The individual eigenvalues were weighted as $w_i = 1/\lambda_i$. Both molecules were treated essentially the same and are discussed together.

The large factor group splitting in both adducts necessitated averaging of observed peak positions between infrared and Raman spectra. In addition, those fundamentals which were split in either the Raman or the infrared spectra were first averaged. The value for ν_2 of the hydrogen-containing isotopic molecules were included in the refinement after correction for Fermi resonance.

Molecular parameters used for the calculation of the G-matrix elements were obtained from two sources. The bond lengths and angles of the methyl portion of the molecule were obtained from Costain.[16] For the BCl_3 adduct the remaining bond parameters were obtained from the structure determination[5] after the symmetry-related bond lengths and angles had been averaged. The B—N, C≡N, and C—C bond lengths for the BBr_3 adduct were assumed to be the same as those found for the BCl_3 adduct. The B—Br bond length

(15) R. G. Snyder and J. H. Schachtschneider, *Spectrochim. Acta*, **19**, 85 (1963); programs GMAT and FPERT (locally modified) were employed: J. H. Schachtschneider, "Vibrational Analysis of Polyatomic Molecules V and VI," Reports 231–64 and 57–65, Shell Development Co., Emeryville, Calif., 1966; program COTRANS also was used: B. Swanson, Ph.D. Thesis, Northwestern University, June 1970.

(16) C. C. Costain, *J. Chem. Phys.*, **29**, 864 (1958).

was obtained by scaling the value found in $Br_3B \cdot N(CH_3)_3$ by the ratio of the B—Cl bond lengths in $Cl_3B \cdot NCCH_3$ and $Cl_3B \cdot N(CH_3)_3$. The BNCC backbone in both molecules was assumed to be linear, and the BBr_3 group was assumed to be tetrahedral. The bonding parameters and symmetry coordinates for both adducts are presented in Table VI.

TABLE VI
MOLECULAR PARAMETERS AND COORDINATES FOR $Cl_3B \cdot NCCH_3$ AND $Br_3B \cdot NCCH_3$

	Bond lengths, Å			Bond angles, deg[a]	
	X = Cl	X = Br		X = Cl	X = Br
r = C—H	1.157	1.157	α = HCH	109.52	109.52
R = B—X	1.825	1.995	β = CCH	109.52	109.52
d = B—N	1.562	1.562	δ = XBX	111.95	109.52
D = C≡N	1.122	1.122	γ = NBX	106.8	109.52
L = C—C	1.437	1.437	ρ = BNC	180.0	180.0
			ϵ = NCC	180.0	180.0

Symmetry Coordinates[b]

A_1 Class

$$S_1 = (1/\sqrt{3})(\Delta r_1 + \Delta r_2 + \Delta r_3)$$
$$S_2 = \Delta D$$
$$S_3 = (1/\sqrt{n_1})[m_1(\Delta\alpha_1 + \Delta\alpha_2 + \Delta\alpha_3) - (\Delta\beta_1 + \Delta\beta_2 + \Delta\beta_3)]$$
$$S_4 = \Delta L$$
$$S_5 = (1/\sqrt{3})(\Delta R_1 + \Delta R_2 + \Delta R_3)$$
$$S_6 = \Delta d$$
$$S_7 = (1/\sqrt{n_2})[m_2(\Delta\gamma_1 + \Delta\gamma_2 + \Delta\gamma_3) - (\Delta\delta_1 + \Delta\delta_2 + \Delta\delta_3)]$$

E Class

$$S_9 = (1/\sqrt{2})(\Delta r_2 - \Delta r_3)$$
$$S_{10} = (1/\sqrt{2})(\Delta\alpha_2 - \Delta\alpha_3)$$
$$S_{11} = (1/\sqrt{2})(\Delta\beta_2 - \Delta\beta_3)$$
$$S_{12} = (1/\sqrt{2})(\Delta R_2 - \Delta R_3)$$
$$S_{13} = \Delta\epsilon$$
$$S_{14} = (1/\sqrt{2})(\Delta\gamma_2 - \Delta\gamma_3)$$
$$S_{15} = (1/\sqrt{2})(\Delta\delta_2 - \Delta\delta_3)$$
$$S_{16} = \Delta\rho$$

[a] See ref 6 for the assumed molecular conformation. [b] $m_1 = -\sqrt{3}\cos\beta/[\cos\alpha/2]$, $n_1 = 3(m_1^2 + 1)$; $m_2 = -\sqrt{3}\cos\gamma/[\cos\delta/2]$, $n_2 = 3(m_2^2 + 1)$.

While the vibrational problem is not grossly underdetermined, the force constant matrix was constrained and only 14 A_1 and 17 E symmetry force constants were included in the calculations of frequencies. The remaining force constants were fixed at values of 0.0, since they involve interactions between symmetry coordinates which do not share a common bond (in the case of stretch–bend or bend–bend interactions) or a common atom (in the case of stretch–stretch interactions).

As described previously for $F_3B \cdot NCCH_3$,[6] interaction constants for the acetonitrile portion of these complexes were transferred from the analysis of liquid acetonitrile. For the BX_3 portion of the molecule it was impossible to refine all of the significant interaction constants; therefore $F_{12,14}$, $F_{12,15}$, and $F_{14,15}$ were constrained to those values found for Cl_3CCCl_3 and Br_3CCBr_3 where the interaction constants have been accurately determined from gas-phase data.[17] The value of $F_{13,16}$ was constrained to 0.05.[18]

Similarly, it was not possible to refine all of the off-diagonal A_1 symmetry force constants, so certain of these were constrained to values which allowed refinement to proceed (Tables VII and VIII). The influence of these interaction constants on the diagonal force constants was carefully investigated for $Cl_3B \cdot NCCH_3$. As expected, the B–N force constant is most sensitive to interaction terms involving the B–N coordinate. The constrained force constants F_{26} and F_{67} were varied over a considerable range without seriously affecting F_{66}.[19] Significantly, the signs of these interaction terms as well as that of F_{56} are correctly reproduced by the usual hybrid orbital arguments.[20] While the influence of off-diagonal terms for $Br_3B \cdot NCCH_3$ was studied in less detail, the same general conclusions apply for F_{66}.

The primary BNC deformation force constant for the BBr_3 adduct was constrained to the value obtained for the BCl_3 adduct, since the frequency for this fundamental was not observed and therefore could not be included in the refinement. The calculated value is *ca.* 70 cm^{-1}.

An attempt was made to find a force field which agreed with the *ca.* 125-cm^{-1} assignment for ν_{16} of the BCl_3 adduct and the *ca.* 110-cm^{-1} assignment for this mode in the BBr_3 adduct. For both molecules the use of these alternate assignments for the BNC deformation

TABLE VII
SYMMETRY FORCE CONSTANTS FOR $Cl_3B \cdot NCCH_3$[a]

A_1 Class

F_{11}	4.93 (2)[b]	F_{77}	1.67 (3)	F_{34}	−0.38 (2)
F_{22}	18.73 (3)	F_{13}	−0.02 (5)	F_{45}	0.0[c]
F_{33}	0.63 (1)			F_{56}	0.78 (10)
F_{44}	5.06 (11)	F_{24}	0.0[c]	F_{57}	−0.7[c]
F_{55}	3.32 (2)	F_{26}	−0.25	F_{67}	0.68[c]
F_{66}	3.40 (16)				

E Class

F_{99}	4.70 (3)	$F_{15,15}$	0.93 (2)	$F_{12,14}$	0.60[c]
$F_{10,10}$	0.56 (1)	$F_{16,16}$	0.26 (9)	$F_{12,15}$	−0.62[c]
$F_{11,11}$	0.69 (1)	$F_{9,10}$	0.26 (4)	$F_{13,16}$	0.08 (8)
$F_{12,12}$	3.25 (4)	$F_{9,11}$	0.09[c]	$F_{14,15}$	0.33[c]
$F_{13,13}$	0.42 (7)	$F_{10,11}$	0.04[c]	$F_{14,16}$	−0.03 (3)
$F_{14,14}$	0.73 (18)	$F_{11,13}$	−0.09[c]		

[a] The subscripts identify F_{kl} with symmetry coordinates k and l as defined in Table VI. Force constants F_{33}, F_{77}, $F_{10,10}$, $F_{11,11}$, $F_{13,13}$ $F_{14,14}$, $F_{15,15}$, $F_{16,16}$, $F_{10,11}$, $F_{14,15}$, $F_{14,16}$, $F_{11,13}$, and $F_{13,15}$ are in units of mdyn Å/(radian)^2 while constants of F_{13}, F_{34}, F_{57}, F_{67}, $F_{9,10}$, $F_{9,11}$, $F_{11,12}$, $F_{12,14}$, and $F_{12,15}$ are in units of mdyn/radian. The remainder are in units of mdyn/Å. [b] Least-squares standard deviations, given in parentheses, represent the deviation in the last decimal place(s) of a given force constant. [c] Force constant constrained.

TABLE VIII
SYMMETRY FORCE CONSTANTS FOR $Br_3B \cdot NCCH_3$[a]

A_1 Class

F_{11}	4.88 (3)[b]	F_{77}	0.98 (4)	F_{34}	−0.38 (5)
F_{22}	18.56 (6)	F_{13}	−0.02 (10)	F_{45}	0.0[c]
F_{33}	0.62 (1)			F_{56}	0.24 (16)
F_{44}	5.05 (26)	F_{24}	0.0[c]	F_{57}	−0.76[c]
F_{55}	2.95 (19)	F_{26}	−0.25[c]	F_{67}	0.33[c]
F_{66}	3.46 (36)				

E Class

F_{99}	4.65 (4)	$F_{15,15}$	1.01 (2)	$F_{12,14}$	0.50[c]
$F_{10,10}$	0.56 (1)	$F_{16,16}$	0.25[c]	$F_{12,15}$	−0.45[c]
$F_{11,11}$	0.70 (1)	$F_{9,10}$	0.29 (6)	$F_{13,16}$	0.15 (7)
$F_{12,12}$	2.61 (13)	$F_{9,11}$	0.09[c]	$F_{14,15}$	0.33[c]
$F_{13,13}$	0.48 (9)	$F_{10,11}$	0.04[c]	$F_{14,16}$	0.06 (16)
$F_{14,14}$	0.67 (43)	$F_{11,13}$	−0.09[c]		

[a] See footnote *a*, Table VII. [b] See footnote *b*, Table VII. [c] Force constant constrained.

(17) For the E symmetry block corresponding force constants from the E_{1g} block of X_3CCX_3 were used: R. A. Carney, E. A. Piotrowsky, A. G. Meister, J. H. Brown, and F. F. Cleveland, *J. Mol. Spectrosc.*, **7**, 209 (1961).

(18) The value for $F_{13,16}$ was obtained by changing this constant so to minimize approximately the correlation of the force constants and obtain a reasonable PED, while maintaining good agreement between the observed and calculated frequencies.

(19) Values were explored for F_{26} ranging from 0.0 to −0.5 and for F_{67} from 0.0 to −1.0. For all of these calculations F_{66} fell into the range 3.38–3.42.

(20) M. I. Mills, *Spectrochim. Acta*, **19**, 1586 (1963).

TABLE IX[a]

OBSERVED AND CALCULATED FUNDAMENTAL FREQUENCIES AND DIFFERENCES FOR FIVE ISOTOPIC VARIETIES OF $Cl_3B \cdot NCCH_3$ (cm^{-1})

	$Cl_3{}^{11}B \cdot NCCH_3$			$Cl_3{}^{11}B \cdot NCCD_3$			$Cl_3{}^{10}B \cdot {}^{15}NCCH_3$			$Cl_3{}^{10}B \cdot NCCH_3$			$Cl_3{}^{10}B \cdot NCCD_3$			
	Obsd	Calcd	Δ	Obsd	Calcd	Δ	Obsd	Calcd	Δ	Obsd	Calcd	Δ	Obsd	Calcd	Δ	PED[d]
$\nu_1(A_1, CH_3$ str)	2931.4	2929.9	1.5	2109.6	2109.5	0.1	2926.3	2929.8	−3.5	2931.2	2929.9	1.3	2110.1[b]	2109.4	0.7	$99V_{11}$
$\nu_2(A_1, C{\equiv}N$ str)	2369.0[c]	2370.0	−1.0	2371.3	2372.5	−1.2	2338.9[c]	2336.5	2.4	2369.9[c]	2370.3	−0.4	2372.0[b]	2372.8	−0.8	$86V_{22}$
$\nu_3(A_1, CH_3$ def)	1356.3	1356.5	−0.2	1105.1	1104.4	0.7	1356.5	1356.5	0.0	1357.0	1356.5	0.5	1105.7[b]	1105.6	0.1	$104V_{33} - 12V_{34}$
$\nu_4(A_1$, C—C str)	1010.2	1010.4	−0.2	925.6	925.0	0.6	1003.5	1005.8	−2.3	1018.0	1016.6	1.4	932.5[b]	933.6	−1.1	$64V_{44} + 36V_{55}$
$\nu_5(A_1$, B—N str)	712.4	709.4	3.0	691.2	689.2	2.0	730.7	735.3	−4.6	734.8	735.6	−0.8	710.4[b]	712.0	−1.6	$17V_{44} + 69V_{55} + 20V_{66} + 65V_{77} - 17V_{56} - 39V_{57} - 21V_{67}$
$\nu_6(A_1, BCl_3$ str)	414.5	413.2	1.3	409.5	411.8	−2.3	414.1	413.2	0.9	413.7	413.4	0.3	409.3[b]	411.9	−2.6	$103V_{66}$
$\nu_7(A_1, BCl_3$ def)	309.5	306.2	3.3	292.5	297.4	−4.9	306.7	305.0	1.7	306.7	306.6	0.1	293.0[b]	297.7	−4.7	$16V_{55} + 59V_{77} + 18V_{57}$
$\nu_9(E, CH_3$ str)	3003.8	3004.8	1.0	2252.0	2250.7	1.3	3004.1	3004.8	−0.7	3003.4	3004.8	−1.4	2252.5	2250.7	1.8	$96V_{99}$
$\nu_{10}(E, CH_3$ def)	1403[b]	1403.6	−0.6	...	1001.4	...	...	1403.5	...	1403.6	1403.6	0.0	...	1001.4	...	$85V_{10,10} + 13V_{11,11}$
$\nu_{11}(E, CH_3$ rock)	1023.7	1027.8	−4.1	844.9	841.2	3.7	1025	1027.6	−2.6	1027.2	1027.8	−0.6	845.2	841.2	4.0	$16V_{10,10} + 76V_{11,11}$
$\nu_{12}(E, BCl_3$ str)	742.3	743.9	−1.6	742.4	743.8	−1.4	771.7	770.7	1.0	772.1	770.8	1.3	770.1	770.1	−0.5	$151V_{12,12} + 12V_{14,14} + 17V_{15,15} - 34V_{12,14} - 36V_{12,15} - 12V_{14,15}$
$\nu_{13}(E$, NCC def)	447.5	450.9	−3.4	431.1	427.6	3.5	441.1	443.5	−2.4	446.1	451.1	−4.4	430.6	427.8	2.8	$10V_{11,11} + 68V_{13,13} + 21V_{14,14} + 46V_{16,16} - 28V_{13,16}$
$\nu_{14}(E, BCl_3$ rock)	261.1	263.7	−2.6	253.6	252.1	1.5	260.7	261.5	−0.8	261.1	263.8	−2.7	256.2	252.1	4.1	$30V_{13,13} + 50V_{14,14} + 11V_{14,15}$
$\nu_{15}(E, BCl_3$ def)	219.0	217.8	1.2	216.5	216.0	0.5	217.7	218.9	−1.2	218.9	219.1	−0.2	216.4	217.4	−1.0	$14V_{12,12} + 42V_{14,14} + 144V_{15,15} + 11V_{16,16} - 19V_{12,14} - 32V_{12,15} - 63V_{14,15}$
$\nu_{16}(E$, BNC def)	...	81.2	...	77.8	72.2	0.6	...	81.2	...	78.9	81.4	−2.5	79.2	77.3	1.9	$19V_{12,12} + 71V_{14,14} + 25V_{15,15} + 46V_{16,16} - 29V_{12,14} - 16V_{12,15} - 34V_{14,16}$

[a] Average deviation: A_1 class, 1.5 cm^{-1}; E class, 3.1 cm^{-1}, for frequencies used in the refinement. $\Delta = \nu(obsd) - \nu(calcd)$. [b] Frequency not included in the refinement. [c] Position corrected for Fermi resonance with $\nu_3 + \nu_4$. [d] Potential energy distribution for the normal isotopic molecule. The subscripts identify V_{kl} with symmetry coordinates kl defined in Table VI. Contributions are expressed as percentages and values less than 10% in magnitude are omitted.

TABLE X[a]

OBSERVED AND CALCULATED FUNDAMENTAL FREQUENCIES AND DIFFERENCES FOR FIVE ISOTOPIC VARIETIES OF $Br_3B \cdot NCCH_3$ (cm^{-1})

	$Br_3{}^{11}B \cdot NCCH_3$			$Br_3{}^{11}B \cdot NCCD_3$			$Br_3{}^{10}B \cdot NCCH_3$			$Br_3{}^{10}B \cdot NCCH_3$			$Br_3{}^{10}B \cdot NCCD_3$			
	Obsd	Calcd	Δ	Obsd	Calcd	Δ	Obsd	Calcd	Δ	Obsd	Calcd	Δ	Obsd	Calcd	Δ	PED[e]
$\nu_1(A_1, CH_3$ str)	2918.2	2915.8	2.4	2103.8	2099.6	4.2	2918.3	2915.8	2.9	2918.3	2915.8	2.5	2106.8[b]	2099.6	7.2	$99V_{11}$
$\nu_2(A_1, C{\equiv}N$ str)	2362.0[c]	2361.6	0.4	2362.5	2364.1	−1.6	2327.2[c]	2328.2	−1.0	2359.0[c]	2361.9	−2.9	2362.2[b]	2364.4	−2.2	$86V_{22}$
$\nu_3(A_1, CH_3$ def)	1351.2	1351.4	−0.2	1106.1	1102.9	3.2	1350.0	1351.3	−1.3	1351.5	1351.4	0.1	1104.5[b]	1104.4	0.1	$104V_{33} + 13V_{34}$
$\nu_4(A_1$, C—C str)	1019.7	1016.3	3.4	935.3	930.1	5.2	1009.6	1012.5	−2.9	1017.5	1023.3	−5.3	943.5[b]	938.9	4.6	$67V_{44} + 38V_{55}$
$\nu_5(A_1$, B—N str)	706.6	695.2	11.4	683.5	671.4	12.1	716.5	718.9	−2.4	720.5	719.2	1.3	698.5[b]	692.2	6.3	$21V_{44} + 69V_{55} + 27V_{66} + 31V_{77} - 38V_{57} - 11V_{67}$
$\nu_6(A_1, BBr_3$ str)	289.9	291.1	−1.2	283.2	284.5	1.3	288.5	290.2	−1.7	289.8	291.5	−1.6	283.2[b]	284.8	−1.6	$12V_{55} + 69V_{66} + 10V_{77} - 10V_{67}$
$\nu_7(A_1, BBr_3$ def)	187.3	188.7	−1.4	185.3	186.8	−1.5	188.0	188.8	−0.8	187.6	189.3	−1.7	186.1[b]	187.4	−1.3	$85V_{77} + 11V_{67}$
$\nu_9(E, CH_3$ str)	2990.5	2992.6	−2.1	2243.7	2243.1	0.6	2991.6	2992.6	−1.0	2990.1	2992.6	−2.5	2244.2	2243.1	1.1	$96V_{99}$
$\nu_{10}(E, CH_3$ def)	1392.2	1391.3	0.9	...[d]	992.4	...	1390.4	1391.3	−0.9	1391.3	1391.3	0.0	...[d]	992.4	...	$84V_{10,10} + 14V_{11,11}$
$\nu_{11}(E, CH_3$ rock)	1031.8	1026.7	5.1	837.4	838.8	−1.4	1017.7	1026.5	−8.8	1031.8	1026.7	5.1	838.0	838.8	−0.8	$17V_{10,10} + 76V_{12,12}$
$\nu_{12}(E, BBr_3$ str)	652.8	650.3	2.5	652.1	650.3	1.8	...[d]	678.7	...	681.0	678.8	2.2	677.9	678.7	−0.8	$139V_{12,12} + 23V_{14,14} + 22V_{15,15} - 43V_{12,14} - 31V_{12,15} - 18V_{14,15}$
$\nu_{13}(E$, NCC def)	428.3	434.2	−5.9	408.4	413.5	−5.1	421.3	426.4	−5.1	426.0	434.2	−8.2	406.8	413.5	−6.7	$83V_{13,13} + 15V_{14,14} + 42V_{16,16} - 53V_{13,16}$
$\nu_{14}(E, BBr_3$ rock)	267.9	265.4	2.5	251.2	248.3	2.9	266.9	262.3	4.6	266.5	265.5	1.0	248.4	248.4	0.0	$39V_{13,13} + 37V_{14,14} + 13V_{13,16}$
$\nu_{15}(E, BBr_3$ def)	144.8	144.2	0.6	144.0	144.1	−0.1	145.3	144.4	0.9	144.1	144.4	−0.3	142.9	144.4	−1.5	$114V_{15,15} - 20V_{14,15}$
$\nu_{16}(E$, BNC def)	...	54.0	...	...[d]	51.2	...	...[d]	54.0	...	...[d]	54.1	...	...[d]	51.2	...	$18V_{12,12} + 100V_{14,14} + 25V_{15,15} + 80V_{16,16} - 32V_{12,14} - 12V_{12,15} - 40V_{14,15} - 29V_{11,13} - 13V_{13,16}$

[a] Average deviation: A_1 class, 2.2 cm^{-1}; E class, 4.1 cm^{-1}, for frequencies used in the refinement. $\Delta = \nu(obsd) - \nu(calcd)$. [b,c] See footnotes *b* and *c* in Table IX. [d] Frequency not observed. [e] Potential energy distribution; see footnote *d* of Table IX.

mode resulted in unrealistic potential energy distributions and poor agreement between observed and calculated frequencies. Also, values for the primary force constants involving the linear angle deformation modes for this force field were unsatisfactory. The Jacobian matrix showed that the low-frequency mode in the E block is affected only by the BNC primary and interaction force constants, and these constants must be changed drastically in order to change the frequency of this mode. Therefore, the original assignment for ν_{16} is preferred.

For the BBr_3 adduct a refinement was made using the *ca.* 125-cm^{-1} assignment for the BBr_3 rock mode, ν_{14}. The lowest value which could be obtained for this mode without introducing large errors in the other frequencies was about 190 cm^{-1}. The PED for this refinement showed an abnormal dependence on interaction constants, and the primary BBr_3 rock force constant was too low. Therefore, the original *ca.* 250-cm^{-1} assignment for ν_{14} is preferred. The final symmetry force constants for the BCl_3 and BBr_3 adducts are presented in Tables VII and VIII, and the final fit between observed and calculated frequencies is given in Tables IX and X.

Discussion

Factor Group Coupling.—While it is peripheral to the main theme of this paper, some interesting spectral details have been observed which may be related to intermolecular coupling and low molecular site symmetry in the solid. For example, the symmetric CH_3 deformation is observed as a sharp doublet for all adducts in the infrared spectrum. However, in the spectrum of 3% $F_3{}^{10}B\cdot NCCH_3$ in a host lattice of $F_3{}^{10}B\cdot NCCD_3$ this mode was observed as a single peak.[6] Apparently, the splitting is destroyed when there is only one hydrogen-containing molecule in the unit cell. This is an example of an A_1 mode which is split by factor group coupling. There are many more examples of E symmetry fundamentals which are split in one or both of the techniques.

Factor group coupling is also responsible for the lack of correspondence between the Raman and infrared positions for many of the fundamentals. The correspondence for the B–N stretch is poor for all the adducts, and for the BCl_3 and BBr_3 adducts the difference between the two techniques is *ca.* 25 cm^{-1}. The same behavior is shown by the symmetric BF_3 stretch and the antisymmetric BCl_3 and BBr_3 stretch modes. For both CH_3 stretching vibrations the correspondence between the infrared and Raman spectra is good for the BF_3 and BCl_3 adducts, but these two techniques give significantly different values for the BBr_3 adduct. Apparently, factor group coupling is more important for the BBr_3 adduct than for the lighter members of the series. The other fundamentals also show that factor group coupling increases going from the BF_3 through the BBr_3 adducts.

One possible origin of the factor group splitting is dipole–dipole interaction in the unit cell which would explain the observed increase in mutual exclusion for the heavier members of the series in terms of the known increase in the dipole moment of the adducts. The packing diagram for the BCl_3 adduct[5] shows that two dipole–dipole interactions are important in the lattice: interaction between molecules in the same plane and interaction between molecules in neighboring planes at $y = {}^1/_4, {}^3/_4$. The latter interaction involves molecules related by a center of symmetry, and in view of the increase in mutual exclusion it is likely that this interaction is becoming more important for the heavier members of the series.

Trends in the Vibrational Frequencies and Force Constants.—Many of the acetonitrile vibrations exhibit large shifts upon adduct formation as well as monotonic shifts in going from the BF_3 through the BBr_3 adducts. The boron halide frequencies are affected considerably by adduct formation; however, simple interpretations of the changes in boron halide frequencies are unreliable because of the extensive mixing of symmetry coordinates in the normal modes.

Following the general trend found for nitriles, the C≡N stretching frequency increases *ca.* 100 cm^{-1} upon adduct formation. The C≡N valence force constant (Table XI) increases significantly upon adduct formation confirming the increase in the C≡N bond strength indicated by the structure data.[6] The increase in the C≡N frequency upon coordination has been attributed to increased C≡N σ-bond strength in the adduct.[21]

TABLE XI
VALENCE FORCE CONSTANTS FOR $X_3B\cdot NCCH_3$

	$NCCH_3$	$F_3B\cdot NCCH_3$	$Cl_3B\cdot NCCH_3$	$Br_3B\cdot NCCH_3$
f_{CN}[a]	17.4	18.8	18.7	18.6
f_{CC}	5.3	5.3	5.1	5.1
f_{BN}	...	2.5	3.4	3.5
f_{NCC}	0.38	0.45	0.41	0.36
f_{BNC}	...	0.20	0.25	0.25

[a] Constants f_{CN}, f_{CC}, and f_{BN} are in units of mdyn/Å while f_{NCC} and f_{BNC} are in units of mdyn Å/(radian)^2.

Both ν_{CN} and the C≡N force constant decrease in going from the BF_3 through the BBr_3 adducts. However, the changes in ν_{CN} are small and the variation in the force constant is not significant since the errors are large. The latter result shows that simple correlations of ν_{CN} are of little value in understanding the bonding in compounds such as these.

Another acetonitrile vibration exhibiting a large shift upon adduct formation is the C–C stretch which is observed to increase *ca.* 60 cm^{-1} in the boron fluoride adduct and *ca.* 100 cm^{-1} in the boron bromide adduct. Whether this increase is partly due to an increase in C–C bond strength cannot be answered at present because both the bond shortening and change in force constant are within the estimated standard deviations. The PED's for the adducts given in Tables IX and X show that the mode assigned to C–C stretch has a large contribution from the B–N stretching force constant and, therefore, the increase in ν_{CC} is partially due to kinematic coupling with B–N stretch. Other changes in the acetonitrile frequencies upon coordination are not large.

For the remaining vibrations the most striking and important change is found for the B–N stretching frequency which increases in the heavier members of the series. The trend is not monotonic since this mode is *ca.* 7 cm^{-1} lower in the BBr_3 adduct than in the BCl_3 adduct. The PED shows that more than one force constant contributes to this normal mode, so a simple

(21) K. F. Purcell and R. S. Drago, *J. Amer. Chem. Soc.*, **88**, 919 (1966); K. F. Purcell, *ibid.*, **89**, 6139 (1967); **90**, 1094 (1968); see, however, K. Kuwai and I. Kanesaka, *Spectrochim. Acta, Sect. A*, **25**, 1265 (1969).

interpretation of frequencies may be misleading, and it is necessary to inspect the B–N force constants for information on the bonding in these molecules. The B–N stretching force constant is *ca.* 0.9 mdyn/Å higher for the BCl_3 adduct than for the BF_3 adduct. While the standard deviations of the two measurements are relatively high, the difference in the force constants is greater than twice the estimated error. Also, as described previously, the constraints used in the normal coordinate do not seriously bias the B–N force constant. Therefore, this difference is considered to be significant, and it is concluded that the B–N bond is stronger in the BCl_3 adduct than in the BF_3 adduct. The B–N force constant for the BBr_3 adduct is slightly smaller than that of the BCl_3 adduct but, in this case, the difference is not significant. Thus, the B–N bond is approximately the same for the boron chloride and boron bromide adducts.

There are indications that in the absence of specific effects, such as steric crowding, the pattern of stronger donor–BCl_3 than donor–BF_3 bond may be general. For example, while they are not conclusive, a variety of older spectroscopic data are consistent with this order of donor–B bond strength.[5] Of particular significance is the recent esr study of nitroxide–boron halide adducts which clearly demonstrates that BCl_3 is a stronger electron acceptor than BF_3.[22]

The BX_3 symmetric and antisymmetric stretching frequencies show the expected decrease in going from the BF_3 through the BBr_3 adducts, and the separation of these two modes increases in the heavier members of the series. Force constants for free BX_3 are compared with those of the adducts in Table XII; the usual decrease in M–X force constants upon adduct formation is observed.[7] In the present case the decrease may in part be attributed to the decrease in BX_3 π bonding upon adduct formation. The largest change is found for the BF_3 adduct which is reasonable since there is more π bonding in BF_3 than in the heavier acids (see below). However, the relative changes are approximate because constraints used in the normal-coordinate treatment affect these particular force constants.

TABLE XII
SYMMETRY VALENCE FORCE CONSTANTS FOR BX_3 STRETCH (MDYN/Å)

	BX_3[a]		$X_3B\cdot NCCH_3$	
	A	E	A	E
F	8.82	7.82	6.49	3.85
Cl	4.63	4.19	3.32	3.24
Br	3.64	2.80	2.94	2.45

[a] I. W. Levin and S. Abramowitz, *J. Chem. Phys.*, **43**, 4213 (1965).

Bonding in $X_3B\cdot NCCH_3$.—The most important aspect of this study is the information it yields concerning the variation in B–N interaction with a change in halogen atom bonded to boron. Any thermodynamic assessment of the B–N bond energy must rely on a variety of uncertain assumptions. Experience has shown that two of the most reliable types of extrathermodynamic information which may be used to infer *relative* bond energies are bond distances and force constants. In previous work on the B–N bond length, it was found that this distance is 0.068 Å shorter for $Cl_3B\cdot NCCH_3$ than for $F_3B\cdot NCCH_3$, and the difference was concluded to be experimentally significant.[5] Similarly, the present work demonstrates a significantly higher (0.9 mdyn/Å) B–N force constant for $Cl_3B\cdot NCCH_3$ than for $F_3B\cdot NCCH_3$. This force constant difference corresponds to about 18 kcal/mol bond energy difference,[23] which is similar to the 8–16 kcal/mol range previously estimated from bond lengths.[5] While the exact values of these bond energy differences are not to be taken seriously, it is significant that two independent estimates indicate that the difference in B–N bond strength between $F_3B\cdot NCCH_3$ and $Cl_3B\cdot NCCH_3$ is of the same magnitude as the difference in the enthalpies of complex formation, 11.8 kcal/mol.[24]

To explore the origin of the stronger B–N bond for the BCl_3 adduct CNDO/2 molecular orbital calculations were performed on BF_3 and BCl_3 with varying degrees of angular distortion.[25] The BCl_3 calculations were carried out with 3s3p and also with 3s3p3d basis orbitals on Cl. The former results appear to be somewhat better;[26] however, they are subject to greater uncertainty than the BF_3 results because CNDO/2 parameters are less reliable for the third period than for lighter elements.

The calculated lowest unoccupied virtual orbital energies, E(LUMO), and total energies, E(total), are presented in Figure 5, which indicates that BCl_3 has a significantly higher electron affinity—lower E(LUMO)—than BF_3.[27] Since the LUMO is primarily localized on boron, the energy of this virtual orbital should give a reasonable indication of the acceptor strength of the boron halide. On this basis it appears that BCl_3 is a stronger electron pair acceptor than BF_3. This difference originates from the smaller degree of B_{p_z}–X_{p_z} interaction for the chloride.

It is clear that upon forming a stable complex the reorganization energy of the BX_3 group must be more than compensated by the donor–acceptor bond energy. These factors are illustrated in Figure 5, which presents

(22) T. B. Eames and B. M. Hoffman, *J. Amer. Chem. Soc.*, in press.

(23) G. W. Chantry, A. Finch, P. N. Gates, and D. Steele, *J. Chem. Soc. A*, 896 (1966).

(24) A. W. Laubengayer and D. S. Sears, *J. Amer. Chem. Soc.*, **67**, 164 (1945).

(25) J. A. Pople and D. L. Beveridge, "Approximate Molecular Orbital Theory," McGraw-Hill, New York, N. Y., 1970. The standard parameters were employed. Boron–halogen distances were held fixed at the experimentally determined bond lengths R(BF) = 1.31 and R(BCl) = 1.75 Å. Program No. 142, QCPE, Indiana University, Bloomington, Ind.

(26) The out-of-plane bending force constant is calculated to be 0.45 mdyn/Å with the sp basis and 0.17 mdyn/Å with an spd basis set for BCl_3. The observed value is 0.42 mdyn/Å: G. Herzberg, "Infrared and Raman Spectra," Van Nostrand, Princeton, N. J., 1945, p 178. From this comparison the sp basis set is preferred. Another check on the calculation is provided by the computed reorganization energy for BF_3, 38 kcal/mol, which compares favorably with 34 kcal/mol from an *ab initio* calculation of D. R. Armstrong and P. G. Perkins, *Chem. Commun.*, 856 (1969). For BCl_3 the calculated reorganization energy is 38 kcal/mol when an sp basis set is used and 11 kcal/mol with an spd basis set. While cross checks between various molecular orbital methods may be provided by comparisons of calculated reorganization energies, the estimation of this quantity is uncertain and the definition is somewhat arbitrary. Therefore calculated reorganization energies do not clarify the subtle differences in acidity between BF_3 and BCl_3.

(27) The difference between E(LUMO) values for planar BCl_3 and BF_3 is 2.3 eV when an sp basis is used for Cl, and it is 3.3 eV when an spd basis is used. For comparison, the top three filled molecular orbitals average about 4.0 eV higher than the three lowest ionization potentials of BF_3: R. J. Boyd and D. C. Frost, *Chem. Phys. Lett.*, **1**, 649 (1968). The three highest filled molecular orbitals of BCl_3 (using either an sp or spd basis set) average about 2.4 eV higher than the corresponding ionization potentials. Thus the highest filled orbitals are calculated to be 1.6 eV too low for BCl_3 relative to BF_3. This error is substantially less than the differences in E(LUMO) between BF_3 and BCl_3, but it can only be concluded that the CNDO/2 *suggests* that BCl_3 has a higher electron affinity than BF_3 because errors in the virtual orbitals are probably higher than for the filled orbitals.

the reorganization energy—change in E(total)—and the acceptor orbital energy—E(LUMO)—for BF_3 and BCl_3 with varying degrees of angular distortion. A striking feature of these results is that the BCl_3 curves are similar to those of BF_3 but shifted to lower energy. When d orbitals are included in the calculation for BCl_3 the total rise in E(total) and drop in E(LUMO) are about one-third of those given in Figure 5 and the curves are shifted to lower energy. While the CNDO/2 calculations are ambiguous concerning reorganization energies, they do indicate that BCl_3 should be a stronger electron acceptor than BF_3 for any degree of reorganization.

In summary, B–N bond length and force constant data indicate that relative B–N bond strengths are of the same order as relative heats of complex formation for $F_3B\cdot NCCN_3$ and $Cl_3B\cdot NCCH_3$. This result is contrary to previous estimates of reorganization energies which indicate that B–N bond strengths are not a determining factor in complex stability and which lead one to the conclusion that donor–acceptor bond energies are actually the reverse of stabilities.[4] We must look to other effects to explain all of the available information on B–N bond lengths, force constants, and heats of complex formation. One alternate explanation of the data, which appears to merit serious consideration, is the interplay between BX_3 reorganization and acceptor strength, such that the most easily reorganized acid (presumably BCl_3) will be distorted to a greater extent and therefore have a greater electron affinity than its less pliable counterpart.[5] Another possible origin of the increased B–N bond strength for the BCl_3 adduct may be the greater electron affinity for BCl_3 than BF_3 due to less p_π–p_π bonding between Cl and B.[28] While the acidity difference between these boron halides is chemically important, it is small enough that a definitive illustration of its origins is beyond the capabilities of current theory, but there is an indication from CNDO calculations that the greater electron affinity of BCl_3 may be a significant factor. It is therefore probable that both factors mentioned above operate in unison to yield a higher acidity for BCl_3 than for BF_3.

Acknowledgment.—We are grateful to the NSF for the support of this work through Grant GP 6676 and to the Advanced Research Projects Agency for support through the Northwestern Materials Research Center. We thank Professor R. C. Taylor for a copy of P. D. H. Clippard's thesis and for helpful correspondence.

(28) While it probably is not decisive, one contribution to the stability trend is an increase in lattice energy for the heavier complexes. The present observation of increasing intermolecular coupling with increasing halide atomic number affords experimental evidence for the expected trend in intermolecular interactions arising from London and polar forces.

CONTRIBUTION FROM THE DEPARTMENT OF CHEMISTRY,
PURDUE UNIVERSITY, WEST LAFAYETTE, INDIANA 47907

Trends in $(CH_3)_2YAuP(C_6H_5)_3$ Compounds ($Y^- = Cl^-, CH_3^-, \sigma\text{-}C_5H_5^-$). Proton Magnetic Resonance and Vibrational Spectra[1]

BY STANLEY W. KRAUHS,[2] GIAN CARLO STOCCO,[3] AND R. STUART TOBIAS*

Received September 2, 1970

The new compounds R_2AuXPR_3 obtained by bridge cleavage of dimethylgold(III) halides can be alkylated cleanly. This method has been used to prepare the known compounds $(CH_3)_3AuP(C_6H_5)_3$ and $(CH_3)_3AuP(C_2H_5)_3$ and the new compound $(\sigma\text{-}C_5H_5)(CH_3)_2AuP(C_6H_5)_3$. Complete laser Raman, infrared, and pmr spectra are given for these compounds as well as for $(CH_3)_2AuClP(C_6H_5)_3$ permitting comparisons in the sequence of compounds $(CH_3)_2YAuP(C_6H_5)_3$ ($Y^- = Cl^-, CH_3^-, \sigma\text{-}C_5H_5^-$). Raman spectra establish that the cyclopentadienyl group in $(C_5H_5)(CH_3)_2AuP(C_6H_5)_3$ is σ bonded, and the pmr spectra establish that it is trans to a methyl group and stereochemically nonrigid as would be expected by analogy with bis(cyclopentadienyl)mercury. Unlike the related $(\sigma\text{-}C_5H_5)(CH_3)_2Tl$, there is no intermolecular exchange of the cyclopentadienyl ligands at 40°. Replacement of Cl^- by CH_3^- leads to a weakening of the Au–C bonds as indicated by a decrease in the frequency of the very intense Au–C stretching bands. Substitution of $\sigma\text{-}C_5H_5^-$ for CH_3^- causes a maximum shift of only 4 cm^{-1} in these frequencies. The trialkyl derivatives show a large trans influence for the alkyl groups leading to a weakening of the mutually trans Au–C bonds.

Introduction

While dialkylgold(III) compounds are among the most stable of the σ-bonded transition metal alkyls, the trialkyl derivatives are considerably less so. Gilman and Woods[4] were able to isolate trimethylgold as the adducts with ethylenediamine, 2-aminopyridine, and benzylamine. These compounds were moderately stable, particularly the ethylenediamine complex, but even it was very light sensitive and detonated upon heating.

Coates and Parkin[5] isolated stable adducts of trimethylgold with trimethyl- and triphenylphosphine either by displacing ethylenediamine from $[(CH_3)_3Au]_2en$ with the phosphine in solution at −20° or by adding the phosphine directly to an ether solution of trimethylgold at −65°. A review of organogold chemistry has appeared recently.[6]

(1) Supported, in part, by Grant GP-23208 from the National Science Foundation. Acknowledgment also is made to the donors of the Petroleum Research Fund, administered by the American Chemical Society for partial support of this research. Presented, in part, at the XIIIth International Conference on Coordination Chemistry, Cracow-Zakopane, Poland, Sept 1970.

(2) NSF undergraduate participant under Grant GY-5845.

(3) Fulbright Fellow from the Institute of General and Inorganic Chemistry, University of Palermo, Palermo, Italy.

(4) H. Gilman and L. A. Woods, *J. Amer. Chem. Soc.*, **70**, 550 (1948).

(5) G. E. Coates and C. Parkin, *J. Chem. Soc.*, 421 (1963).

(6) B. Armer and H. Schmidbaur, *Angew. Chem., Int. Ed. Engl.*, **9**, 101 (1970).